Nanostructures

DOI: 10.1002/anie.200907130

# Carbon-Nanotube-Array Double Helices**

*Qiang Zhang, Meng-Qiang Zhao, Dai-Ming Tang, Feng Li, Jia-Qi Huang, Bilu Liu, Wan-Cheng Zhu, Ying-Hao Zhang, and Fei Wei**

The helix is a geometric motif that can be found in both natural and artificial structures. Helicity can be observed in the spiral arms of galaxies or in microscopic structures, such as right- or left-handed quartz, as well as in human art and architecture. The double-helix structure, which consists of two congruent helices with the same axis or differing by a translation along the axis, is the basic structure of deoxyribonucleic acid (DNA).[1] Recently, helical supramolecules, such as double-stranded helical oligonuclear coordination compounds and biomolecules, have been synthesized and they exhibit amazing electron-transfer, magnetic, and sensor properties.[2,3] Double-helix nanoarchitecture is still a new world to be explored. Until now, the helix structure could only be constructed by conformational restrictions of the macromolecules, inter- or intramolecular hydrogen bonds, or coordination to metal ions.[3] It is still a great challenge to realize the feasible self-organization of thousands of nanowires/nanotubes into a double-helix structure during the formation process.

The use of carbon nanotubes (CNTs) as promising building blocks for the single/double-helix structure provides a novel platform for demonstrating the superior electronic, mechanical, and thermal properties of one-dimensional (1D) nanomaterials. Great efforts have recently been made to study single-helical carbon nanofibers (CNFs)[4] and nanotubes[5] because of their coiled morphologies and potential applications. Helical CNTs have been demonstrated to show unique electrical[6,7] and mechanical properties[8] that are useful for potential applications in nanoengineering. For example, by applying an electric current through a helical CNT, an inductive magnetic field can be generated. This indicates that the helical CNTs can be used as electromagnetic nanotransformers and nanoswitches.

Depending upon the location of pentagons and heptagons, a helical CNT can behave as a metal, a semiconductor, or a semimetal.[6] If there is a sharp density-of-state peak at the Fermi level, the helical CNTs can even show superconducting properties, as predicted by tight-binding models.[6] Their potential applications span high-frequency electronics, tactile and magnetic sensors, and structural foams for cushioning and energy dissipation.[6–8] Up to now, single-helical CNTs have generally been synthesized as by-products in the catalytic decomposition of organic substances over transition-metal catalysts or their alloys.[5,9] The synthesis of CNT-array double helices, similar to organic forms found in nature (e.g., DNA and proteins), remains a challenge.

Generally, the formation of the double-helix structure requires self-organization of two strands with one end as the node. If aligned CNTs are oppositely grown on a single flake, then the two strands may coil on themselves around the flake and twist into a double helix. Based on this consideration, we explored the idea of bottom-up growth of aligned CNTs on a layered double hydroxide (LDH) flake to form a CNT-array double helix directly. The LDHs are a class of synthetic two-dimensional (2D) nanostructured anionic clays, the structure of which can be described as containing brucite-like layers in which a fraction of the divalent cations coordinated octahedrally by hydroxy groups have been replaced isomorphously by trivalent cations, to give positively charged layers with charge-balancing anions between them. Some hydrogen-bonded water molecules may occupy any remaining free space in the interlayer region.

LDHs can be represented by the general formula $M^{2+}_{1-x}M^{3+}_{x}(OH)_2A^{n-}_{x/n}\cdot m\,H_2O$ ($M^{2+}=Mg^{2+}$, $Fe^{2+}$, $Co^{2+}$, $Ni^{2+}$, $Cu^{2+}$, or $Zn^{2+}$, for example; $M^{3+}=Al^{3+}$, $Cr^{3+}$, $Mn^{3+}$, $Fe^{3+}$, or $Ga^{3+}$, for example) with the value of $x$ being equal to the molar ratio of $M^{3+}/(M^{2+}+M^{3+})$ (generally within the range 0.2–0.33).[10] Compared with planar substrates (e.g., wafer, quartz plate, glass) which were widely used as substrates for the growth of aligned CNTs, LDH flakes exhibit some extraordinary properties; for instance, a single LDH flake is very light ($\approx$0.2 ng), and metal dispersion is at an atomic level with controllable components.[10] High-density metal particles can be provided for aligned CNT growth. Herein, LDH flakes directly served as 2D flat substrates for the self-organization of CNT-array double helices during growth by chemical vapor deposition (CVD). Moreover, the electrical performance of the CNT-array double helix was measured, and the conductivity could be readily modulated by densification of the CNTs in the double helix.

[*] Dr. Q. Zhang, Dr. M. Q. Zhao, J. Q. Huang, Dr. W. C. Zhu, Y. H. Zhang, Prof. F. Wei
Beijing Key Laboratory of Green Reaction Engineering and Technology
Department of Chemical Engineering, Tsinghua University
Beijing 100084 (China)
Fax: (+86) 10-6277-2051
E-mail: wf-dce@tsinghua.edu.cn
Dr. D. M. Tang, Prof. F. Li, B. L. Liu
Shenyang National Laboratory for Materials Science
Institute of Metal Research
Chinese Academy of Sciences, 72 Wenhua Road
Shenyang 110016 (China)

[**] We thank Prof. Hui-Ming Cheng and Dr. Wei-Zhong Qian for fruitful discussions and valuable suggestions. This work was supported by the National Natural Science Foundation of China (No. 20736004, 20736007, 2007AA03Z346) and the China National Nanotechnology Program (No. 2006CB0N0702).

Supporting information for this article is available on the WWW under http://dx.doi.org/10.1002/anie.200907130.

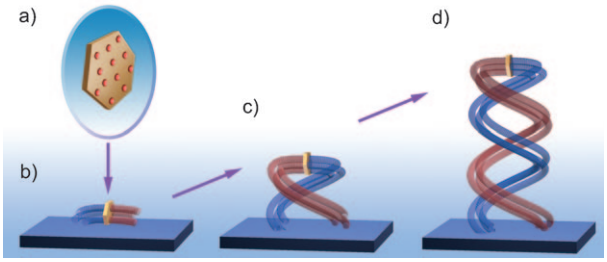


***Figure 1.*** Formation of the CNT-array double helix. An Fe(Co)/Mg/Al LDH flake was used as the substrate. For details, see text.

Our concept involved the facile CVD growth of CNT-array double helices on an LDH flake, as illustrated in Figure 1 and demonstrated by the video in the Supporting Information. LDH flakes served directly as 2D lamellar substrates. Active catalyst nanoparticles with a high density were formed on both sides of the flake after calcination and reduction (Figure 1 a). After the introduction of a carbon source at high temperature, aligned CNTs grew synchronously on both sides of the flake. When the CNT tips met space resistance, the as-grown CNT strands twisted and self-organized into a double-helix structure (Figure 1 b–d).

As shown in Figure 2 a, a large amount of loose Fe/Mg/Al LDH flakes were synthesized to serve as substrate and catalyst precursor. CNT-array double helices were formed during CVD growth (Figure 2 b). There were close-packed dextrorotatory (Figure 2 c–e) and levorotatory (Figure 2 f,g) helical CNT strands, in both of which CNT arrays were uniformly twisted with each other. A flake could be found at the end of each CNT-array double helix (arrows), which connected the two CNT strands. The as-grown CNTs were self-organized into CNT-array double helices. Moreover, the screw pitch of the dextrorotatory and levorotatory double helix could be stretched from 3 to 10 μm (Figure 2 h and i). This method can be generalized to synthesize a family of CNT-array double helices using various LDH flakes (e.g., Co/Mg/Al, Fe/Co/Mg/Al LDH flakes; see the Supporting Information, Figure S1).

The structure of the CNTs in the double helix can be easily modulated by varying the active sites on the flakes. Typical TEM images of the as-grown CNT products in the double helices grown on LDH flakes are shown in Figure 3 and Figure S2 in the Supporting Information. When Fe/Mg/Al (0.4:2:1) LDHs were used as catalysts, double-walled CNTs (> 95 %) with an inner diameter of 4–6 nm were synthesized. Few encapsulated catalyst particles were found in the inner core of the as-grown CNTs. In contrast, few-walled CNTs with a wall number ranging from 3 to 6 were obtained when Co/Fe/Mg/Al (0.2:0.2:2:1) LDHs served as the catalyst (Figure S2 in the Supporting Information). Compared with double/few-walled CNTs grown from porous Fe/MgO, CNTs in the double helix contained more defects within the structure, which possibly results from the regular insertion of pentagon–heptagon pairs.

Helical CNTs were generally synthesized as by-products on Fe/In, Fe/Sn, and Fe/Ni catalysts, most of which were single helices.[5,9,11] In some cases, two helical CNFs with a diameter

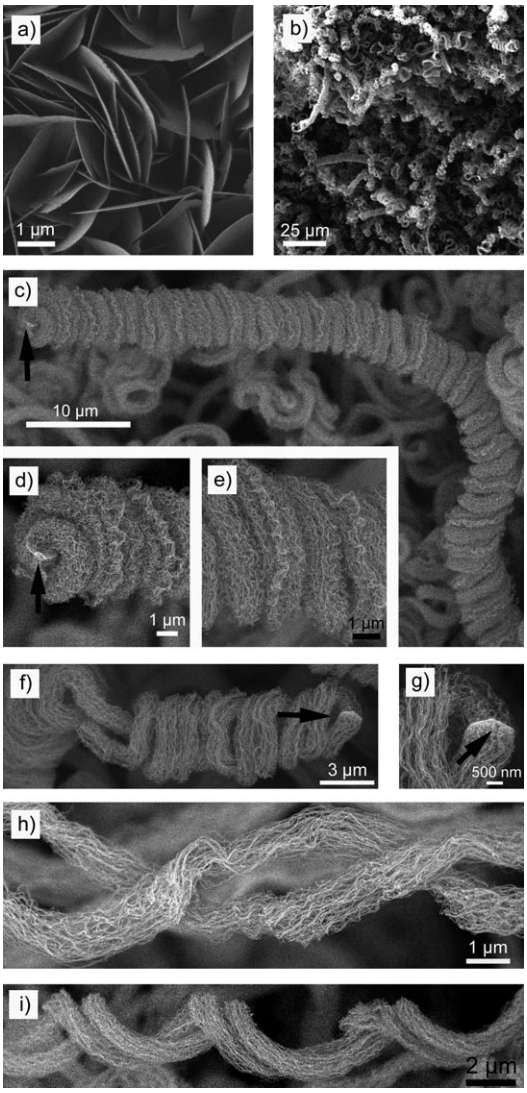


***Figure 2.*** CNT-array double helices grown on Fe/Mg/Al LDH flakes. a) As-obtained Fe/Mg/Al LDH flakes; b) a large number of CNT-array double helices; c) dextrorotatory CNT-array double helices grown on LDH flakes; d,e) calcined LDH flakes and middle section of (c); f) levorotatory double helix grown on an LDH flake; g) high-magnification image of the catalyst position in (f); stretched h) levorotatory and i) dextrorotatory CNT-array double helices. The arrows in (c), (d), (f), and (g) indicate calcined LDH flakes.

of approximately 100 nm grew on one Fe nanoparticle.[11] The morphologies of these previously reported helical CNTs and CNFs[5,9,11] are quite different from the present double-helix structure. On the other hand, although a few other reports have described the growth of CNTs on LDH flakes,[12] only entangled CNTs among flakes were obtained.[12] Aligned CNTs can be intercalated among lamellar substrates.[13] Recently, it was also reported that aligned CNTs could be grown on floating substrates,[14] but the flakes were prepared by roll-to-roll electron-beam evaporation rather than chemical routes and the CNT strands only grew on one side of the flakes. Therefore, this is the first report of the unprecedented self-organization of CNTs into an ordered three-dimensional (3D) double-helix structure on a simple flake.

  

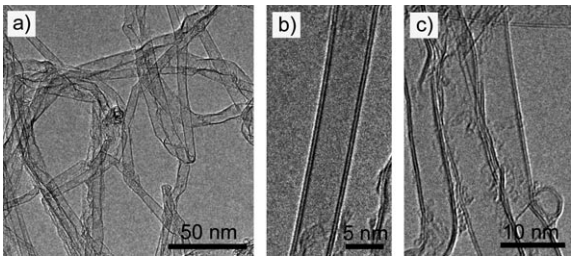


***Figure 3.*** a) TEM and b,c) high-resolution TEM images of double-walled CNTs grown on a single Fe/Mg/Al LDH flake.

The successful growth of CNT-array double helices on LDH flakes was mainly attributed to the following factors. At the beginning, metal-catalyst particles can be formed in high density on both sides of the LDH flakes after $H_2$ reduction. As illustrated in Figure 4a, Fe nanoparticles with a size distribution of 4–7 nm and a density of about $5\times10^{15}\,m^{-2}$ were formed on Fe/Mg/Al (0.4:2:1) LDH flakes. With the introduction of a carbon source, aligned CNTs can synchronously grow and extend on both sides of the LDH flakes (Figure 4b). One intrinsic feature of the growth of CNT arrays from a LDH flake is the freedom to grow in such a way as to minimize the stresses associated with the growth of a CNT strand. Thus, when CNT arrays met space resistance (such as neighboring flakes, CNT arrays, or the wall of the reactor), the arrays coiled on themselves around the flakes (Figure 4c,d). The arrays can twist in a left- or right-handed way, thus leading to the formation of CNT-array double helices (Figure 4d).

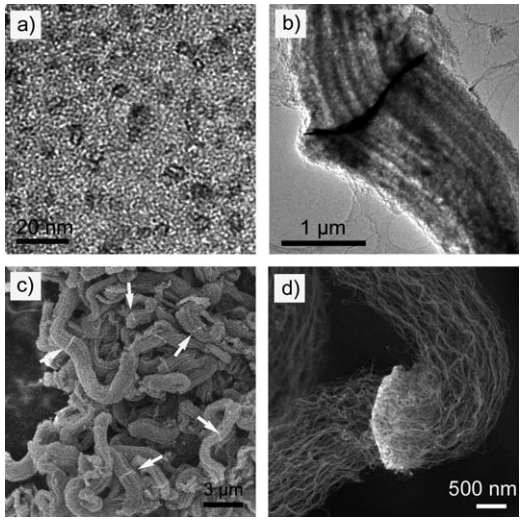


***Figure 4.*** a) Metal-catalyst particles on a calcined Fe/Mg/Al LDH flake. b) CNT arrays oppositely grown on an Fe/Mg/Al LDH flake. c) Short CNT arrays grown on Fe/Mg/Al LDH flakes; the arrows indicate calcined LDH flakes. d) Twisting of CNT arrays for continuous growth of a CNT double helix.

It is the LDH flake that provides an ultralight substrate with high-density catalyst particles on each side for the simultaneous growth of CNT strands, so that the coiling and further twisting become much easier. Moreover, the twisting can take place continuously upon rotating the catalyst flake, thus leading to the formation of long CNT double helices. The unprecedented self-organization mode releases the stress easily, and overcomes the diffusion limitation of the carbon source for growth of superlong double helices. Furthermore, the handedness of each CNT strand must be the same because both strands were grown on the same flake. If the handedness of one strand changed, the other must be altered simultaneously to minimize the stresses (Figure S3 in the Supporting Information). Interestingly, in some cases we found that even six CNT strands grown on three LDH flakes can twist into CNT gyros (Figure S4 in the Supporting Information).

The electrical performance of the CNT-array double helix was characterized in situ inside a scanning electron microscope at room temperature by using a nanoprobe system. As demonstrated in the inset of Figure 5a, probe A was in contact with two arrays, whereas probes B and C just pressed on different individual CNT arrays. By addition of a positive or negative voltage on probes B and C, electron currents between probes A/B and A/C were detected that were as high as $1.8\times10^{6}$ and $-1.0\times10^{6}$ nA, respectively. Although the double-helical CNTs were twisted, the current was inverse, which provides a prototype for nanoelectromagnetic Faraday coils for nanoelectromechanical systems. However, the magnetic field was estimated to be about $1\times10^{-4}$ T (current: 1 mA), which was too weak to induce the movement of CNT strands in the double helix.

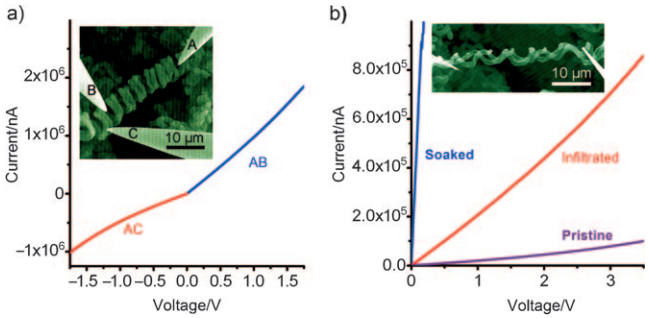


***Figure 5.*** a) Inverse voltages applied to each CNT array in a double helix. b) Current–voltage (*I*–*V*) curves of pristine, infiltrated, and soaked CNT-array double helices.

If the double-helical CNT array was infiltrated in a drop of ethanol for 1 min, or soaked in ethanol for 10 min, the double-helix morphology was well preserved but the diameter of the arrays decreased. When a voltage of 0.15 V was applied to pristine, infiltrated, and soaked CNT-array double helices, the current density increased from $8.6\times10^{4}$ to $9.5\times10^{5}$ and $2.9\times10^{7}\,A\,cm^{-2}$, respectively (Figure 5b). Similar to CNT yarns tightened by ethanol,[15] the CNT strands in the double helix were also densified by capillary forces during solvent evaporation, and the contact resistance among the CNTs decreased, thus leading to high current density at the same applied voltage. However, there is still scope for further exploration from the fact that metallic nanotubes can carry an electrical current density of $4\times10^{9}\,A\,cm^{-2}$.[16]

  

In summary, we have demonstrated the synthesis of CNT-array double helices on LDH flakes through a novel self-organization process during in situ CVD growth. The structure of both CNTs and strands is controllable. The as-grown CNT arrays in the double helix are able to carry high current, and the electrical conductivity can be further modulated. This is a novel facile route to build 3D double-helix nanoarchitectures by bottom-up self-organization between 1D nanowires/nanotubes and 2D flakes/films, which is suitable for large-scale production. More applications could be opened up if the enhanced electrical, magnetic, mechanical, and optical properties of CNT-array double helices were fully exploited. This work also provides a structural platform towards the design of hierarchical materials that can be used in areas such as nanoelectronics, magnetic devices, catalysis, separation, and energy conversion.

## Experimental Section

Catalyst preparation: The Fe/Mg/Al LDH flakes were prepared by a urea-assisted co-precipitation reaction. $Mg(NO_3)_2{\cdot}6H_2O$, $Al(NO_3)_3{\cdot}9H_2O$, and urea were dissolved in deionized water (250.0 mL) with $[Mg^{2+}]+[Al^{3+}]=0.15\ mol\,L^{-1}$, $n(Mg):n(Al)=2:1$, and $[urea]=3.0\ mol\,L^{-1}$. $Fe(NO_3)_3{\cdot}9H_2O$ was then dissolved in the solution, and the molar ratio of Fe to Al was controlled at 0.4. The as-obtained solution was kept at 105 °C under continuous magnetic stirring for 12 h in a 500 mL flask (equipped with a reflux condenser) under ambient atmosphere. Then the prepared suspension was kept at 95 °C for another 12 h without stirring. After filtering the mixture and washing and freeze-drying the residue, the final products were ground to give brown-yellow powders. The other types of LDH flakes were prepared by the same process, for which the compositions were fixed as $n(Co):n(Mg):n(Al)=0.4:2:1$ and $n(Co):n(Fe):n(Mg):n(Al)=0.2:0.2:2:1$.

Synthesis of CNT-array double helices: In a catalytic CVD process, the LDH catalyst (about 20 mg) was sprayed uniformly onto a quartz plate, which was then placed at the center of a horizontal quartz tube (inner diameter of 25 mm), which was inserted into a furnace at atmosphere pressure. The furnace was heated under flowing Ar ($300\ mL\,min^{-1}$). When the temperature reached 750 °C, the flow rate of the Ar was reduced to $100\ mL\,min^{-1}$ and maintained for 10 min. $C_2H_4$ ($300\ mL\,min^{-1}$) was introduced into the reactor 5 min before the introduction of $H_2$ ($50\ mL\,min^{-1}$). Growth was maintained for 30 min at 750 °C before the furnace was cooled to room temperature under Ar protection. Samples were then collected for further analysis and tests.

Characterization: The morphology of the CNT-array double helix was characterized by using a JSM 7401F scanning electron microscope operated at 3.0 kV, and a JEM 2010 high-resolution transmission electron microscope operated at 120.0 kV. The *I–V* measurements were performed at room temperature in a vacuum better than $1\times10^{-6}$ Torr using a MM3A-nanoprobe system (Kleindiek) installed in a scanning electron microscope (FEI NanoSEM430).

Received: December 17, 2009
Published online: April 7, 2010

**Keywords:** carbon · chemical vapor deposition · helical structures · nanotubes · self-assembly

[1] a) J. D. Watson, F. H. C. Crick, *Nature* **1953**, *171*, 737; b) M. Albrecht, *Chem. Rev.* **2001**, *101*, 3457.
[2] a) J. M. Lehn, *Angew. Chem.* **1990**, *102*, 1347; *Angew. Chem. Int. Ed. Engl.* **1990**, *29*, 1304; b) N. Kobayashi, T. Naito, T. Inabe, *Adv. Mater.* **2004**, *16*, 1803.
[3] a) C. Piguet, G. Bernardinelli, G. Hopfgartner, *Chem. Rev.* **1997**, *97*, 2005; b) X. M. Chen, G. F. Liu, *Chem. Eur. J.* **2002**, *8*, 4811; c) T. Hasegawa, Y. Furusho, H. Katagiri, E. Yashima, *Angew. Chem.* **2007**, *119*, 5989; *Angew. Chem. Int. Ed.* **2007**, *46*, 5885; d) J. Z. Hou, M. Li, Z. Li, S. Z. Zhan, X. C. Huang, D. Li, *Angew. Chem.* **2008**, *120*, 1735; *Angew. Chem. Int. Ed.* **2008**, *47*, 1711.
[4] a) S. Motojima, Y. Itoh, S. Asakura, H. Iwanaga, *J. Mater. Sci.* **1995**, *30*, 5049; b) S. Motojima, S. Asakura, T. Kasemura, S. Takeuchi, H. Iwanaga, *Carbon* **1996**, *34*, 289; c) Y. K. Wen, Z. M. Shen, *Carbon* **2001**, *39*, 2369; d) S. Yang, X. Chen, M. Kusunoki, K. Yamamoto, H. Iwanaga, S. Motojima, *Carbon* **2005**, *43*, 916; e) D. M. Tang, C. Liu, F. Li, W. C. Ren, J. H. Du, X. L. Ma, H. M. Cheng, *Carbon* **2009**, *47*, 670.
[5] a) S. Amelinckx, X. B. Zhang, D. Bernaerts, X. F. Zhang, V. Ivanov, J. B. Nagy, *Science* **1994**, *265*, 635; b) H. Q. Hou, Z. Jun, F. Weller, A. Greiner, *Chem. Mater.* **2003**, *15*, 3170; c) J. N. Wang, L. F. Su, Z. P. Wu, *Cryst. Growth Des.* **2008**, *8*, 1741; d) W. Wang, K. Q. Yang, J. Gaillard, P. R. Bandaru, A. M. Rao, *Adv. Mater.* **2008**, *20*, 179.
[6] K. Akagi, R. Tamura, M. Tsukada, S. Itoh, S. Ihara, *Phys. Rev. Lett.* **1995**, *74*, 2307.
[7] A. Volodin, D. Buntinx, M. Ahlskog, A. Fonseca, J. B. Nagy, C. Van Haesendonck, *Nano Lett.* **2004**, *4*, 1775.
[8] a) R. B. Pipes, P. Hubert, *Compos. Sci. Technol.* **2002**, *62*, 419; b) M. Lu, K. T. Lau, J. C. Xu, H. L. Li, *Colloids Surf. A* **2005**, *257–258*, 339; c) X. Q. Chen, S. L. Zhang, D. A. Dikin, W. Q. Ding, R. S. Ruoff, L. J. Pan, Y. Nakayama, *Nano Lett.* **2003**, *3*, 1299.
[9] a) L. J. Pan, T. Hayashida, A. Harada, Y. Nakayama, *Phys. B* **2002**, *323*, 350; b) J. Liu, S. Webster, D. L. Carroll, *Appl. Phys. Lett.* **2006**, *88*, 213119; c) D. W. Li, L. J. Pan, J. Qian, D. Liu, *Carbon* **2010**, *48*, 170; d) N. J. Tang, Y. Yang, K. J. Lin, W. Zhong, C. T. Au, Y. W. Du, *J. Phys. Chem. C* **2008**, *112*, 10061; e) N. J. Tang, W. Zhong, C. T. Au, Y. Yang, M. G. Han, K. J. Lin, Y. W. Du, *J. Phys. Chem. C* **2008**, *112*, 19316.
[10] a) D. G. Evans, D. A. Xue, *Chem. Commun.* **2006**, 485; b) D. P. Debecker, E. M. Gaigneaux, G. Busca, *Chem. Eur. J.* **2009**, *15*, 3920.
[11] N. J. Tang, W. Zhong, C. T. Au, A. Gedanken, Y. Yang, Y. W. Du, *Adv. Funct. Mater.* **2007**, *17*, 1542.
[12] a) F. Li, Q. Tan, D. G. Evans, X. Duan, *Catal. Lett.* **2005**, *99*, 151; b) H. I. Hima, X. Xiang, L. Zhang, F. Li, *J. Mater. Chem.* **2008**, *18*, 1245; c) Y. Zhao, Q. Z. Jiao, C. H. Li, J. Liang, *Carbon* **2007**, *45*, 2159; d) R. Benito, M. Herrero, F. M. Labajos, V. Rives, C. Royo, N. Latorre, A. Monzon, *Chem. Eng. J.* **2009**, *149*, 455; e) L. Zhang, F. Li, X. Xiang, M. Wei, D. G. Evans, *Chem. Eng. J.* **2009**, *155*, 474; f) M. Q. Zhao, Q. Zhang, X. L. Jia, J. Q. Huang, Y. H. Zhang, F. Wei, *Adv. Funct. Mater.* **2010**, *20*, 677.
[13] a) Q. Zhang, M. Q. Zhao, Y. Liu, A. Y. Cao, W. Z. Qian, Y. F. Lu, F. Wei, *Adv. Mater.* **2009**, *21*, 2876; b) Q. Zhang, M. Q. Zhao, J. Q. Huang, J. Q. Nie, F. Wei, *Carbon* **2010**, *48*, 1196; c) D. S. Su, *ChemSusChem* **2009**, *2*, 1009.
[14] C. L. Pint, S. T. Pheasant, M. Pasquali, K. E. Coulter, H. K. Schmidt, R. H. Hauge, *Nano Lett.* **2008**, *8*, 1879.
[15] X. B. Zhang, K. L. Jiang, C. Teng, P. Liu, L. Zhang, J. Kong, T. H. Zhang, Q. Q. Li, S. S. Fan, *Adv. Mater.* **2006**, *18*, 1505.
[16] S. J. Kang, C. Kocabas, T. Ozel, M. Shim, N. Pimparkar, M. A. Alam, S. V. Rotkin, J. A. Rogers, *Nat. Nanotechnol.* **2007**, *2*, 230.

  